

Distributed Optimization in Sensor Network for Scalable Multi-Robot Relative State Estimation

Tianyue Wu and Fei Gao

Abstract—This paper is dedicated to achieving scalable relative state estimation using inter-robot Euclidean distance measurements. We consider equipping robots with distance sensors and focus on the optimization problem underlying relative state estimation in this setup. We reveal the commonality between this problem and the coordinates realization problem of a sensor network. Based on this insight, we propose an effective unconstrained optimization model to infer the relative states among robots. To work on this model in a distributed manner, we propose an efficient and scalable optimization algorithm with the classical *block coordinate descent* method as its backbone. This algorithm exactly solves each block update subproblem with a closed-form solution while ensuring convergence. Our results pave the way for distance measurements-based relative state estimation in large-scale multi-robot systems.

I. INTRODUCTION

There is a growing consensus that a large-scale multi-robot system can be more robust, resilient, and efficient in achieving goals that would be difficult to achieve with a single robot [1], [2]. These multi-robot missions often require individuals with knowledge of each other’s pose and location relative to their own (known as the *relative state* [3]–[8]) to collaborate on the downstream tasks [9]–[11].

Although there have been prior works devoted to the problem of relative state estimation in multi-robot systems, they either employ a straightforward centralized approach [3]–[5] or require the incorporation of the robot’s self-localization information (e.g., from odometry) [6]–[8]. On the one hand, in large-scale deployments, centralized schemes present communication challenges due to the need for frequent data aggregation and synchronized transmission, leading to communication congestion and delays. Moreover, these schemes miss out on the benefits of distributed computing, such as parallelism and workload sharing. On the other hand, schemes that incorporate self-localization usually have a *persistent excitation* [12] requirement for observability, limiting the feasibility of such approaches. As the scale of the system grows, continuous transmission of self-localization data can also become a non-negligible burden, as claimed in [13]. These factors collectively contribute to a pessimistic expectation of adopting these approaches when deploying multi-robot systems at scale.

Fortunately, the last two decades have witnessed a series of studies on the problem of recovering *realizations* of a large set of points in \mathbb{R}^d , which best explain their relative Euclidean distances [14]. These studies provide

intuition for equipping (possibly multiple) distance sensors on each robot and using inter-robot distance measurements to achieve *scalable* relative state estimation. By characterizing the relative state of the robots with sensors’ point coordinates, we can relate the relative state estimation problem to the rich literature on points realization problems such as sensor network localization [15]–[18], molecular conformation [19]–[21], and so on. Accordingly, we propose a nonlinear programming (NLP) model for the estimation problem derived from the coordinates of sensors, as well as a *block coordinate descent* (BCD) [22] method for distributed local searching on the model.

We summarize our contributions as follows:

- 1) We present a novel perspective for the distance measurements-based relative state estimation problem by transforming it into a problem that finds realizations of a robotic sensor network.
- 2) We propose an effective unconstrained NLP model for the transformed problem, which encourages using the BCD method, a natural choice for distributed settings and scalable optimization, to solve it.
- 3) We design a specialized BCD-type algorithm called *Burer-Monteiro factorization with Block Coordinate Descent* (BM-BCD) that performs exact block updates to work on the proposed NLP model efficiently.

We perform extensive numerical experiments on the proposed optimization model and algorithm. The encouraging results validate the potential of using distance sensors for scalable relative state estimation.

II. FROM RELATIVE STATE ESTIMATION TO REALIZATION OF SENSOR NETWORK

In this section, we specify the setup of distance measurements-based relative state estimation and transform the underlying optimization problem (Problem 1) into one of finding realizations of a sensor network (Problem 2).

A. Problem Setup and Preliminaries

Consider a multi-robot system with n members equipped with distance sensors (e.g., Ultra-WideBand sensors) and being able to obtain accurate estimates of their pitch angle ϕ and roll angle θ (e.g., from Inertial Measurement Unit as in previous works [7], [8]) if the system acts in space ($d = 3$), rather than in a plane ($d = 2$). To ensure that the relative states are observable in most cases, each robot is equipped with *two* distance sensors¹ that form a (robotic)

¹Note that the results in the latter sections can be extended to heterogeneous configurations, where the number of distance sensors on different robots varies, requiring only additional considerations of observability [3].

sensor network to infer the relative states across the entire system according to the inter-robot distance measurements.

We specify a *common reference system* shared by the whole system, in which the robots' states and the coordinates of the sensors are expressed. This reference system can be set arbitrarily when $d = 2$, while its z-axis should be aligned with the opposite direction of gravity when $d = 3$.

We model the measurements topology underlying the problem using an undirected graph $\mathcal{G} = (\mathcal{V}, \mathcal{E})$ in which each node $i \in \mathcal{V}$ represents one robot in the system and the edges $(i, j) \in \mathcal{E}$ indicate that the measurements between robots i, j are taken into account in the estimation problem. A binary set $\mathcal{B} := \{0, 1\}$ is introduced to distinguish between two distance sensors on a robot. Let $\mathbf{p} := [p_1^0, p_1^1, p_2^0, p_2^1, \dots, p_n^0, p_n^1] \in \mathbb{R}^{d \times 2n}$ denote a realization of the sensor network in \mathbb{R}^d . The component $p_i^u := [x_i^u; y_i^u] \in \mathbb{R}^2$ or $p_i^u := [x_i^u; y_i^u; z_i^u] \in \mathbb{R}^3$ for $i = 1, 2, \dots, n$ and $u \in \mathcal{B}$, is the coordinate of sensor (i, u) . We have the following measurement model:

$$\tilde{d}_{ij}^{uv} = \underline{d}_{ij}^{uv} + \epsilon = \left\| \underline{p}_i^u - \underline{p}_j^v \right\| + \epsilon, \quad \epsilon \sim \mathcal{N}(0, \sigma^2), \quad (1)$$

$$\forall (i, j) \in \mathcal{E}, \quad u, v \in \mathcal{B},$$

where ϵ is the measurement noise and σ is the noise level. For optimization reasons, we use the following quadratic model [23] to approximate (1):

$$\tilde{q}_{ij}^{uv} := \left(\tilde{d}_{ij}^{uv} \right)^2 - \sigma^2 \simeq \left(\underline{d}_{ij}^{uv} \right)^2 + \epsilon_{ij}^{uv}, \quad \epsilon_{ij}^{uv} \sim \mathcal{N}(0, (\sigma_{ij}^{uv})^2),$$

$$\sigma_{ij}^{uv} = \sqrt{(2\sigma \underline{d}_{ij}^{uv})^2 + 2\sigma^4}, \quad \forall (i, j) \in \mathcal{E}, \quad u, v \in \mathcal{B}. \quad (2)$$

Letting $\underline{R}_i, \underline{t}_i$ represent the rotation and translation components of the robot i 's state in the common reference system and \underline{p}_i^u the coordinate of sensor u on the robot i in its body reference system, we immediately have

$$\underline{p}_i^u = \underline{R}_i \underline{p}_i^u + \underline{t}_i. \quad (3)$$

Given a set of noisy measurements according to the topology \mathcal{G} , it is straightforward to show the maximum-likelihood estimation (MLE) model for 3D relative state estimation based on inter-robot distance measurements:

Problem 1 (MLE model for Euclidean distance-based relative state estimation).

$$\min_{\{(R_i, t_i)\}} \sum_{\substack{(i, j) \in \mathcal{E} \\ u, v \in \mathcal{B}}} \frac{1}{(\sigma_{ij}^{uv})^2} \left(\|R_i \underline{p}_i^u + t_i - R_j \underline{p}_j^v - t_j\|^2 - \tilde{q}_{ij}^{uv} \right)^2, \quad (4)$$

s.t.

$$R_i = R_{i|z} \tilde{R}_{i|y} \tilde{R}_{i|x} = \begin{bmatrix} \cos \psi_i & -\sin \psi_i & 0 \\ \sin \psi_i & \cos \psi_i & 0 \\ 0 & 0 & 1 \end{bmatrix} * \quad (5)$$

$$\begin{bmatrix} \cos \tilde{\phi}_i & 0 & \sin \tilde{\phi}_i \\ 0 & 1 & 0 \\ -\sin \tilde{\phi}_i & 0 & \cos \tilde{\phi}_i \end{bmatrix} * \begin{bmatrix} 1 & 0 & 0 \\ 0 & \cos \tilde{\theta}_i & -\sin \tilde{\theta}_i \\ 0 & \sin \tilde{\theta}_i & \cos \tilde{\theta}_i \end{bmatrix},$$

where $\tilde{\phi}_i$ and $\tilde{\theta}_i$ are the (known) accurate estimates of pitch and roll angles, while ψ_i is the yaw angle to be estimated. By removing (5), it is straightforward to obtain the 2D analogy of Problem 1.

B. Transformation of Problem 1

Next we will show that the sensor coordinates $\{(p_i^u, p_i^v)\}$ are in one-to-one correspondence with the states $\{(\underline{R}_i, \underline{t}_i)\}$. Firstly, we have

$$p_i^u - p_i^v = R_i (\bar{v}_i^u - \bar{v}_i^v)$$

$$= \begin{bmatrix} \cos \psi_i & -\sin \psi_i & 0 \\ \sin \psi_i & \cos \psi_i & 0 \\ 0 & 0 & 1 \end{bmatrix} * \left(\tilde{R}_{i|y} \tilde{R}_{i|x} (\bar{v}_i^u - \bar{v}_i^v) \right). \quad (6)$$

Introducing $[\bar{v}_{i|x}; \bar{v}_{i|y}; \bar{v}_{i|z}] := \tilde{R}_{i|y} \tilde{R}_{i|x} (\bar{v}_i^u - \bar{v}_i^v)$ for the sake of concise writing, a straightforward computation shows the following relations from the first two rows of (6):

$$\sin \psi_i = \frac{(\bar{v}_{i|x} (y_i^u - y_i^v) - \bar{v}_{i|y} (x_i^u - x_i^v))}{\left(\bar{v}_{i|x}^2 + \bar{v}_{i|y}^2 \right)}, \quad (7)$$

$$\cos \psi_i = \frac{(\bar{v}_{i|x} (x_i^u - x_i^v) + \bar{v}_{i|y} (y_i^u - y_i^v))}{\left(\bar{v}_{i|x}^2 + \bar{v}_{i|y}^2 \right)}, \quad (8)$$

which means that we can recover a unique R_i by $\{(p_i^u, p_i^v)\}$ and then recover a unique t_i from (3). So far a one-to-one correspondence between $\{(p_i^u, p_i^v)\}$ and $\{(\underline{R}_i, \underline{t}_i)\}$ is found.

Now it is ready to establish the MLE model based on the coordinates of the sensor network. Since ψ will be redundant in this model, we integrate (7), (8) together with the last row of (6) using $\sin^2 \psi_i + \cos^2 \psi_i = 1$, to obtain a pair of compact relational equations that are equivalent to (5), as follows:

$$\|p_i^u - p_i^v\| = \|\bar{v}_i^u - \bar{v}_i^v\|,$$

$$z_i^u - z_i^v = [-\sin \tilde{\phi}_i, \cos \tilde{\phi}_i \sin \tilde{\theta}_i, \cos \tilde{\phi}_i \cos \tilde{\theta}_i] (\bar{v}_i^u - \bar{v}_i^v).$$

As the last step, we replace the variables in the objective function that represent robots' states with the coordinates of sensors using (3), thereby obtaining the following problem:

Problem 2 (MLE model for robotic sensor network localization).

$$\min_{\mathbf{p}} \sum_{\substack{(i, j) \in \mathcal{E} \\ u, v \in \mathcal{B}}} \frac{1}{(\sigma_{ij}^{uv})^2} \left(\|p_i^u - p_j^v\|^2 - \tilde{q}_{ij}^{uv} \right)^2, \quad (9)$$

s.t.

$$\|p_i^u - p_i^v\| = \|\bar{v}_i^u - \bar{v}_i^v\|, \quad \forall i \in \mathcal{V}, u, v \in \mathcal{B}, u < v, \quad (10)$$

$$z_i^u - z_i^v = [-\sin \tilde{\phi}_i, \cos \tilde{\phi}_i \sin \tilde{\theta}_i, \cos \tilde{\phi}_i \cos \tilde{\theta}_i] (\bar{v}_i^u - \bar{v}_i^v), \quad \forall u, v \in \mathcal{B}, u < v. \quad (11)$$

Problem 2 shares the same objective function as the (anchor-free) noisy *sensor network localization* (SNL) problem [16], which aims to find the realization that best explains the noisy measurements of a sensor network, while constraints (10), (11) are not present in the original SNL problems. We note that a 2D analogy of Problem 2 can be obtained by simply removing the constraint (11).

C. Problem 2 as Rank-constrained SDP

Problem 2 allows a rank-constrained semidefinite programming (SDP) formulation with a corresponding relaxed SDP problem [15]. To reveal this, variable X is critically introduced as follows:

$$X := \mathbf{p}^T \mathbf{p}. \quad (12)$$

The above substitution is equivalent to

$$X \succeq \mathbf{p}^T \mathbf{p}, \quad \text{rank}(X) \leq d,$$

and thus can be rewritten as follows [24]:

$$Z := \begin{bmatrix} X & \mathbf{p}^T \\ \mathbf{p} & I_d \end{bmatrix} \succeq 0, \quad \text{rank}(Z) \leq d. \quad (13)$$

It is readily shown that

$$\begin{aligned} \|p_i^u - p_j^v\|^2 &= Z_{2i-1+u, 2i-1+u} - Z_{2i-1+u, 2j-1+v} \\ &\quad - Z_{2j-1+v, 2i-1+u} + Z_{2j-1+v, 2j-1+v} = \mathcal{A}_{ij}^{uv} \cdot X, \end{aligned} \quad (14)$$

$$z_i^u - z_i^v = X_{2n+3, 2i-1+u} - X_{2n+3, 2i-1+v} = \mathcal{A}_{i|z} \cdot X, \quad (15)$$

where operator \mathcal{A}_{ij}^{uv} and $\mathcal{A}_{i|z}$ are defined to capture the above linear mapping. From above, it is directly to declare that Problem 2 can be formulated as a SDP with a rank constraint appearing in (13), as follows:

Problem 3 (Rank-constrained SDP for Problem 2).

$$\min_Z \sum_{\substack{(i,j) \in \mathcal{E} \\ u,v \in \mathcal{B}}} \frac{1}{(\sigma_{ij}^{uv})^2} (\mathcal{A}_{ij}^{uv} \cdot Z - \tilde{q}_{ij}^{uv})^2, \quad (16)$$

$$\text{s.t.} \quad Z := \begin{bmatrix} X & \mathbf{p}^T \\ \mathbf{p} & I_d \end{bmatrix} \succeq 0, \quad \text{rank}(Z) \leq d.$$

$$\mathcal{A}_{ii}^{uv} \cdot Z = \|\bar{v}_i^u - \bar{v}_i^v\|^2, \quad \forall i \in \mathcal{V}, u, v \in \mathcal{Z}, u < v, \quad (17)$$

$$\mathcal{A}_{i|z} \cdot Z = [-\sin \tilde{\phi}_i, \cos \tilde{\phi}_i \sin \tilde{\theta}_i, \cos \tilde{\phi}_i \cos \tilde{\theta}_i] (\bar{v}_i^u - \bar{v}_i^v), \quad \forall u, v \in \mathcal{B}, u < v. \quad (18)$$

A standard approach to rank-constrained SDP in related problems is to drop out the rank constraint, solve the SDP relaxation, and obtain a high-rank Z (in the presence of noise, the rank of Z is often much larger than d). Afterward, the estimate is extracted from Z either (i) (anchored case:) from the (2, 1)-th block of the Z in (13) [15], [16] or (ii) (anchor-free case:) by performing an eigenvalue decomposition on X to obtain an approximate low-rank solution [20], [21].

However, neither of the methods of extracting estimates is applicable to our problem. On the one hand, since there is no anchor in our situation, extracting the estimates directly from the matrix blocks will yield an erroneous realization crowded toward the origin, as claimed in [20], [21]. On the other hand, the approach via eigenvalue decomposition will somewhat lose the first-order information from (11), again resulting in erroneous estimates. Moreover, as a semidefinite programming, the relaxation of Problem 3 can in principle be solved in polynomial time using interior point methods [25]; however, the high computational cost and the centralized nature of generic semidefinite programming algorithms can limit their scalability in practice. To overcome the dilemma above, a nonlinear programming model is proposed as an effective alternative to Problem 3 in the next section.

III. A NONLINEAR PROGRAMMING MODEL FOR ROBOTIC SENSOR NETWORK LOCALIZATION

In this section, we propose an unconstrained nonlinear programming (NLP) model that facilitates using the block coordinate descent (BCD) algorithm for efficient solutions. Instead of dropping out the rank constraint and directly processing the high-dimensional matrix Z , we follow the

proposal of Burer and Monteiro [26], [27] to factorize Z with some low-rank rectangular matrices $Y \in \mathbb{R}^{r \times (2n+d)}$:

$$Z = Y^T Y = \begin{bmatrix} U^T \\ Q^T \end{bmatrix} [U \quad Q], \quad Q^T Q = I_d, \quad (19)$$

where $U \in \mathbb{R}^{r \times 2n}$ and $Q \in \mathbb{R}^{r \times d}$ with r satisfying $d \leq r \leq 2n + d$, being the rank upper bound we impose on Z . This directly produces an NLP model that (i) implies a constraint on the rank of Z rather than ignoring it, (ii) has a significantly lower dimension of the optimization variable relative to Z as long as we take $r \ll n$, and (iii) leaves the explicit positive semidefiniteness constraint redundant since $Y^T Y \succeq 0$, which is shown as follows:

$$\min_{U, Q} \sum_{\substack{(i,j) \in \mathcal{E} \\ u,v \in \mathcal{B}}} \frac{1}{(\sigma_{ij}^{uv})^2} \left(\mathcal{A}_{ij}^{uv} \cdot \begin{bmatrix} U^T \\ Q^T \end{bmatrix} [U \quad Q] - \tilde{q}_{ij}^{uv} \right)^2, \quad (20)$$

$$Q^T Q = I_d, \quad (21)$$

with constraints (17), (18) where Z is replaced with U, Q by analogy with (20).

Next, motivated by additional computational considerations, a more tractable model is built on top of (20):

Fixing the projection operator: As seen from the constitutive relation from U, Q to Z , $Q^T U$ is actually a surrogate of the realization \mathbf{p} . Therefore, Q can be considered as a (row) projection operator that maps the variable U onto the realization space \mathbb{R}^d .

In the proposed NLP model, we choose a specific Q and fix it throughout the optimization procedure. As a result, our model does not maintain the orthogonality constraint (21)². Note that with Q fixed, different choices of Q do not intrinsically affect the model's behavior, so we can trivially determine Q as $[I_d \quad \mathbf{0}_{d \times (r-d)}]^T$, for example.

Approximating the equality constraints: We propose to simply employ a quadratic penalty method [29, Chapter 17.1] to approximate the equality constraints and reformulate the NLP model (20) as an (approximate) unconstrained alternative. See Problem 4 for an ex-ante insight.

Specifically, the approximation is achieved by adding to the objective function the following penalty terms that replace constraints (17) and (18), respectively:

$$\frac{1}{(\sigma_{i|v})^2} \left(\mathcal{A}_{ii}^{uv} \cdot \begin{bmatrix} U^T \\ Q^T \end{bmatrix} [U \quad Q] - dv_i \right)^2, \quad (22)$$

$$\frac{1}{(\sigma_{i|z})^2} \left(\mathcal{A}_{i|z} \cdot \begin{bmatrix} U^T \\ Q^T \end{bmatrix} [U \quad Q] - dz_i \right)^2, \quad (23)$$

where

$$dv_i = \|\bar{v}_i^u - \bar{v}_i^v\|^2, \quad (24)$$

$$dz_i = [-\sin \tilde{\phi}_i, \cos \tilde{\phi}_i \sin \tilde{\theta}_i, \cos \tilde{\phi}_i \cos \tilde{\theta}_i] (\bar{v}_i^u - \bar{v}_i^v), \quad (25)$$

²Although whether Q is fixed or not has no effect on the optimal values of the model and the corresponding estimates, it does not mean that both nonlinear programming models will produce the same behavior and achieve the same estimate in the local search process. There is no theoretical evidence to compare the estimation accuracy of the two models. Still, the optimization procedure of the model with fixed Q is expected more efficient since no preserving of orthogonality constraint [28] is required.

and the penalty coefficients $\sigma_{i|\nu}$ and $\sigma_{i|z}$ are parameters set to be small relative to the noise level σ_{ij}^{uv} . A *continuation* mechanism is co-designed in the algorithm (Section IV, Algorithm 1) with the penalty terms to achieve accurate estimates while performing considerable efficiency.

Introducing difference into the factors: A recent work [30] provides strong theoretical guarantees for solving *block multiconvex* [30, Sec. 1] problems with the cyclic BCD algorithm. These results increase the confidence in using BCD methods to solve such problems. With these findings, authors in [18] demonstrated how to construct the block multiconvex problem by introducing *difference* into the factors Y^T and Y in the Burer-Monteiro factorization (19), and take advantages of such difference in optimization. Specifically, factorization (19) can be rewritten as

$$Z = Y^T Y = \begin{bmatrix} U^T \\ Q^T \end{bmatrix} [V \quad Q], \quad U = V, \quad Q^T Q = I_d. \quad (26)$$

The difference constraint $U = V$ is added to the objective function as a penalty term $\gamma * \|U - V\|_F^2$, where γ is a penalty coefficient. So far, we have obtained the following unconstrained NLP model the proposed BCD algorithm finally works on:

Problem 4 (Unconstrained nonlinear programming model for robotic sensor network localization).

$$\begin{aligned} \min_{U \in \mathbb{R}^{r \times 2n}} F(U, V) = & \sum_{\substack{(i,j) \in \mathcal{E} \\ u,v \in \mathcal{B}}} \frac{1}{(\sigma_{ij}^{uv})^2} \left(\mathcal{A}_{ij}^{uv} \cdot \begin{bmatrix} U^T \\ Q^T \end{bmatrix} [V \quad Q] - \tilde{q}_{ij}^{uv} \right)^2 \\ & + \sum_{i \in \mathcal{V}} \frac{1}{(\sigma_{i|\nu})^2} \left(\mathcal{A}_{ii}^{uv} \cdot \begin{bmatrix} U^T \\ Q^T \end{bmatrix} [V \quad Q] - d\nu_i \right)^2 \\ & + \sum_{i \in \mathcal{V}} \frac{1}{2(\sigma_{i|z})^2} \left(\mathcal{A}_{i|z} \cdot \begin{bmatrix} V^T \\ Q^T \end{bmatrix} [U \quad Q] - dz_i \right)^2 \\ & + \sum_{i \in \mathcal{V}} \frac{1}{2(\sigma_{i|z})^2} \left(\mathcal{A}_{i|z} \cdot \begin{bmatrix} U^T \\ Q^T \end{bmatrix} [V \quad Q] - dz_i \right)^2 + \gamma \|U - V\|_F^2. \end{aligned} \quad (27)$$

We note that a 2D analogy of the model can be obtained by removing the terms in F derived from (23).

We summarize the main intentions of introducing such a difference as follows:

(i) The form of F allows obtaining a closed-form solution (Proposition 1) efficiently for each *block update subproblem* in the BCD framework when a reasonable block division (as will be explained in Section IV) is applied.

(ii) Under reasonable block division, the objective function F is block multiconvex. In particular, each block update subproblem is strongly convex to meet Assumption 2 of [30]. Therefore, some good convergence properties proposed in [30] can be established for the proposed BCD algorithm (Theorem 1).

IV. BURER-MONTEIRO FACTORIZATION WITH BLOCK COORDINATE DESCENT (BM-BCD)

To take advantage of the formal features of F and to support distributed settings, we develop a specialized NLP

Algorithm 1 Burer-Monteiro factorization with Block Coordinate Descent (BM-BCD)

Parameter: Dimension d , rank r , projection operator Q , initial penalty coefficients $\sigma_{i|\nu}^{(1)}$ and $\sigma_{i|z}^{(1)}$, number of continuation iterations N_c , update factor μ_l and μ_z

Input: Block division $\{\Phi_q\}$, initialization $U^{(0)} = V^{(0)}$,

Output: Robots' states estimates $\{(\hat{R}_i, \hat{t}_i)\}$

```

1:  $k \leftarrow 0$ 
2: // Dynamic- $\gamma$  iterations
3: calculating  $\gamma^{(1)}$ 
4: while 1 do
5:    $k \leftarrow k + 1$ 
6:   for  $q = 1, \dots, p$  do
7:     for  $(i, u) \in \Phi_q$  parallelly do
8:        $(U_i^u)^{(k)} \leftarrow \text{BlockUpdate}U((i, u))$ 
9:     end for
10:    end for
11:    for  $q = 1, \dots, p$  do
12:      for  $(i, u) \in \Phi_q$  parallelly do
13:         $(V_i^u)^{(k)} \leftarrow \text{BlockUpdate}V((i, u))$ 
14:      end for
15:      end for
16:      if  $\frac{F^{(k-1)} - F^{(k)}}{F^{(k-1)}} < \epsilon_F$  or
           $\max \left\{ \frac{4\|U^{(k)} - V^{(k)}\|_F}{\|U^{(k)}\|_F + \|V^{(k)}\|_F}, \frac{\|U^{(k)} - U^{(k-1)}\|_F}{\|U^{(k-1)}\|_F}, \frac{\|V^{(k)} - V^{(k-1)}\|_F}{\|V^{(k-1)}\|_F} \right\} < \epsilon$  then
17:         $(U^{(k)}, V^{(k)}) \leftarrow \left( \frac{U^{(k)} + V^{(k)}}{2}, \frac{U^{(k)} + V^{(k)}}{2} \right)$ 
18:        calculating  $\gamma_{\text{final}}$  and fixing  $\gamma$  as  $\gamma_{\text{final}}$ 
19:        break
20:      else
21:         $\gamma^{(k+1)} \leftarrow \text{Update}\gamma$ 
22:      end if
23:    end while
24: selecting  $i$  and fixing coordinates of sensors  $(i, 0)$  and  $(i, 1)$ 
25: // Continuation iterations
26: for  $N = 1, \dots, N_c$  do
27:   while 1 do
28:     lines 5-15
29:     if  $\max \left\{ \frac{\|U^{(p)} - U^{(p-1)}\|_F}{\|U^{(p-1)}\|_F}, \frac{\|V^{(p)} - V^{(p-1)}\|_F}{\|V^{(p-1)}\|_F} \right\} < \epsilon$  then
30:        $(U^{(k)}, V^{(k)}) \leftarrow \left( \frac{U^{(k)} + V^{(k)}}{2}, \frac{U^{(k)} + V^{(k)}}{2} \right)$ 
31:        $\sigma_{i|\nu}^{(N+1)} \leftarrow \sqrt{\mu_l} * \sigma_{i|\nu}^{(N)}, \sigma_{i|z}^{(N+1)} \leftarrow \sqrt{\mu_z} * \sigma_{i|z}^{(N)}$ 
32:       break
33:     end if
34:   end while
35: end for
36: // Refinement
37: if  $r > d$  then
38:    $r \leftarrow d$ 
39:    $(U^{(k)}, V^{(k)}) \leftarrow \left( Q^T \frac{U^{(k)} + V^{(k)}}{2}, Q^T \frac{U^{(k)} + V^{(k)}}{2} \right)$ 
40:    $Q \leftarrow I_d$ 
41:   do lines 2-34
42: end if
43: recover  $\{(\hat{R}_i, \hat{t}_i)\}$  from  $U^{(k)}$  according to (3), (7) and (8)

```

algorithm with the classical BCD method as its backbone. We call the proposed algorithm *Burer-Monteiro factorization with Block Coordinate Descent* (BM-BCD, Algorithm 1).

Firstly, we formalize the *block update subproblem* in the BCD framework of our problem. Let *block division* $\{\Phi_q\}_{q=1,\dots,p}$ be subsets of the sensors' ID $\mathbb{S} = \{(i, u)\}_{i=1,\dots,n, u=0,1}$ such that $\bigcup_{q=1}^p \Phi_q = \mathbb{S}$ and $\bigcap_{q=1}^p \Phi_q = \emptyset$. Variables belonging to block Φ_q are optimized in the following subproblem

$$\min_{U_q} F_{U|q}(U_q) := F\left(U_q, \hat{U}_{\mathbb{S}\setminus\Phi_q}, \hat{V}\right), \quad (28)$$

where U_q is a component of U , which surrogates realizations of the sensors indexed by the elements in Φ_q , while $\hat{U}_{\mathbb{S}\setminus\Phi_q}$ and \hat{V} are the fixed values of the remaining blocks. The block update subproblems for variables in V are constructed in the same way as (28). At this point, we are ready to explain each component of the proposed algorithm and provide corresponding theoretical results following [18], [30].

Exact block update: In BM-BCD, the block updates (for example, line 8 of Algorithm 1) are performed by solving (28) exactly. More precisely, the update subproblem w.r.t. variable U_i^u which is the $2i - 1 + u$ column of U (and is actually a surrogate for the realization of sensor (i, u)) for any $1 \leq i \leq n$ and $u \in \{0, 1\}$, can be solved exactly in a closed-form. This result is formalized as follows:

Proposition 1. Fix other columns of U as well as the variable V arbitrarily. The solution of the block update subproblem (28) w.r.t. U_i^u are $(U_i^u)^* = (A_{i|d}^u + A_{i|\nu}^u + A_{i|z}^u + A_{i|\gamma}^u)^{-1}(b_{i|d}^u + b_{i|\nu}^u + b_{i|z}^u + b_{i|\gamma}^u)$ and $(U_i^u)^* = (A_{i|d}^u + A_{i|\nu}^u + A_{i|\gamma}^u)^{-1}(b_{i|d}^u + b_{i|\nu}^u + b_{i|\gamma}^u)$ for 3D and 2D problem respectively, where

$$\begin{aligned} A_{i|d}^u &= \sum_{\substack{j \in \mathcal{N}_i \\ v \in \mathcal{B}}} \frac{1}{(\sigma_{ij}^{uv})^2} (V_i^u - V_j^v) (V_i^u - V_j^v)^T, \\ b_{i|d}^u &= \sum_{\substack{j \in \mathcal{N}_i \\ v \in \mathcal{B}}} \frac{1}{(\sigma_{ij}^{uv})^2} \left[(V_i^u - V_j^v)^T U_j^v + \tilde{q}_{ij}^{uv} \right] (V_i^u - V_j^v), \\ A_{i|\nu}^u &= \frac{1}{(\sigma_{i|\nu})^2} (V_i^u - V_i^v) (V_i^u - V_i^v)^T, \quad (v=1-u) \\ b_{i|\nu}^u &= \frac{1}{(\sigma_{i|\nu})^2} \left[(V_i^u - V_i^v)^T U_i^v + d\nu_i \right] (V_i^u - V_i^v), \quad (v=1-u) \\ A_{i|z}^u &= \frac{1}{2(\sigma_{i|z})^2} Q \begin{bmatrix} 0 & 0 & 0 \\ 0 & 0 & 0 \\ 0 & 0 & 1 \end{bmatrix} Q^T, \\ b_{i|z}^u &= \frac{1}{2(\sigma_{i|z})^2} \left(\begin{bmatrix} 0 \\ 0 \\ 1 \end{bmatrix}^T Q^T U_i^v + (v-u) dz_i \right) Q \begin{bmatrix} 0 \\ 0 \\ 1 \end{bmatrix}, \quad (v=1-u) \\ A_{i|\gamma}^u &= \gamma I_d, \quad b_{i|\gamma}^u = \gamma V_i^u. \end{aligned}$$

By swapping the positions of U and V in the above equations, it is direct to obtain the updates of columns in V .

According to Proposition 1, the closed-form update only requires solving a low-dimensional linear system (with its dimension being $r \ll n$), so the exact updates have superior

or comparable efficiency to the approximate ones. Meanwhile, since exact updates achieve the largest reduction of the overall cost function, fewer iterations are required than those algorithms with approximate updates, suppose that the algorithm converges. The following results show that each iteration of continuation (lines 27-34) and the refinement step (lines 36-42) of Algorithm 1 do converge and converge to a stationary point of F with fixed penalty coefficients.

Assumption 1. Every sensor point is connected, directly or indirectly, to at least one sensor with a fixed coordinate.

Theorem 1. Fix $\sigma_{i|\nu}$, $\sigma_{i|z}$ and γ . Let $(U^{(p)}, V^{(p)})$ be the p -th iteration generated by BCD method with exact updates and \mathcal{N} the set of stationary points of F . Under Assumption 1 and block division ensuring that each update subproblem is strongly convex with positive modules [30, Sec. 2], we have

$$\lim_{p \rightarrow \infty} \text{dist} \left((U^{(p)}, V^{(p)}), \mathcal{N} \right) = 0.$$

Proof. Assumption 1 implies that the level set $\{(U, V) \mid F(U, V; \gamma) \leq \alpha\}$ of F is bounded [15, Proposition 1]. Therefore, the boundness of the sequence $\{(U^{(p)}, V^{(p)})\}$ and the existence of a Nash equilibrium can be guaranteed according to Remark 2.4 and Remark 2.2 of [30], respectively. For every block to which the exact update [30, Eq.(1.3a)] is applied, the subproblem is strongly convex (with a constant modulus $\frac{1}{(\sigma_{i|z})^2} + 2\gamma$ under block division mentioned immediately below) so that the Assumption 2 of [30] is satisfied. Then Corollary 2.4 of [30] directly shows that the sequence converges to a Nash equilibrium of F , which must be one of the stationary points of F as claimed in Remark 2.2 of [30].

Note that in the context of our problem, Assumption 1 does not generally hold because the knowledge of sensors' absolute locations are not necessary for relative state estimation. Still, we can artificially fix the coordinates of two sensors on a particular robot (as performed in line 24) without losing generality but guaranteeing the convergence.

Block division: Proposition 1 and the proof of Theorem 1 demonstrate the necessity of dividing variables in U and V into separate blocks for block strong convexity of F and to enable closed-form updates. To achieve this, a reasonable block division scheme is to split each column of U and V into $2 \times 2n$ blocks. These column-wise blocks can be further combined for parallel execution using a natural method called graph coloring [22, Chapter 1.2.4]. A coloring scheme is provided for the *dependency graph* that captures the dependencies relationship between variables. When two variables are independent of each other in their respective block update subproblems, meaning that the (fixed) value of one variable does not affect the solution of the update subproblem for the other variable, they can be assigned the same color and enter the same block.

Remarkably, there are distributed algorithms available that can greedily identify a $(\Delta + 1)$ -colors scheme for an arbitrary graph [31], where Δ denotes the maximum degree of the graph. As the multi-robot system scales up, Δ can be controlled to remain nearly constant. In this case, the number

of blocks is almost invariant to the scale of the system.

Remark 1 (BCD method: a natural choice for distributed settings and scalable optimization). To advance the BCD procedure, each robot i only needs to solve the block update subproblems w.r.t. the sensors on it and communicate locally with its neighbors \mathcal{N}_i . Moreover, BCD can be easily executed in parallel and are suitable for asynchronous implementation, with the number of blocks depending on the maximum degree of \mathcal{G} . This fact implies that, ideally, the time taken for optimization and the communication overhead per iteration are somewhat independent of the system's scale.

Dynamic- γ iterations: The choice of γ may have a significant impact on the number of iterations required for BM-BCD. Therefore, additional maintenance of γ is necessary as the price for introducing difference. We (currently) adopt the method described in [18] to calculate (lines 3 and 18) and update (line 21) γ during the first few iterations of the algorithm. We note that since line 16 of Algorithm 1 limits the reduction rate of F , the termination of dynamic- γ iterations can be guaranteed by the lower boundedness of F .

Continuation iterations: An imitation of *continuation* [32] is designed in BM-BCD compared to the vanilla BCD algorithm. This mechanism is implemented in the loop of line 26 in Algorithm 1 and the update of penalty coefficients in line 31. It follows that the mechanism serves to iteratively improve the feasibility of the solution found by the approximate NLP model w.r.t. the equality constraints (17) and (18). We note that fixing μ_l and μ_z to very small values throughout the algorithm makes updating difficult (imagine that only the penalty terms come into play during the optimization process), and in this case, the algorithm finally terminates in the vicinity of the initialization.

Remark 2 (Penalty coefficients of BM-BCD). The initial penalty coefficients $\sigma_{i|\nu}^{(1)}$, $\sigma_{i|z}^{(1)}$ have to be chosen judiciously. Here we provide a method of calculating these coefficients that works well in practice:

$$\sigma_{i|\nu}^{(1)} = 0.2 * d\nu_i, \quad (29)$$

$$\sigma_{i|z}^{(1)} = \left(\frac{\partial dz}{\partial \phi} \Big|_{\tilde{\phi}_i} + \frac{\partial dz}{\partial \theta} \Big|_{\tilde{\theta}_i} \right) * \frac{\pi}{45}, \quad (30)$$

where $dz(\phi, \theta)$ is a multivariate function constructed by replacing $\tilde{\phi}_i$ and $\tilde{\theta}_i$ in (25) with variables ϕ and θ , respectively. We also found that in the case that we take μ_l and μ_z as $1/10 \sim 1/50$ (which is commonly used in continuation methods), the number of iterations N_c set as $2 \sim 3$ is sufficient to achieve an accurate estimate.

Refinement: Local refinement has been widely used in SNL and molecular conformation problems. Starting from the estimate given by the upstream algorithm, the refinement stage uses a standard centralized nonlinear optimization method to find a stationary point of the objective function. Suppose that r is chosen to be exactly the dimension d in our NLP model, U (or V) itself can be considered a realization of the sensor network. Accordingly, we propose to emulate a distributed refinement step by setting $r = d$ and $Q = I_d$ as performed in lines 35-41 of Algorithm 1.

Problem	d	n	max degree / min degree
CUBE (Fig. 2(a))	3	l^3	26 / 7 ($n \geq 3$)
PYRAMID (Fig. 2(b))	3	$\sum_{i=1}^l \sum_{j=1}^i j$	24 / 6 ($n \geq 3$)
HEXAGON (Fig. 2(c))	2	$6 \times \sum_{i=1}^l i + 1$	12 / 5 ($n \geq 3$)
RECTANGLE (Fig. 2(d))	2	$l \times 2l$	8 / 5 ($n \geq 3$)

Table 1. Information of the 4 simulation problems.

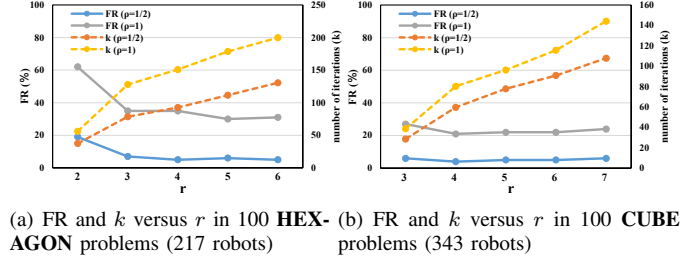


Figure 1. Parametric testing of r on 2D and 3D problems.

V. NUMERICAL EXPERIMENTS

We perform evaluations of the proposed NLP model with BM-BCD algorithm working on it in numerical simulations. Our simulation consists of four simulation problems, where the robots respectively form a 3D cube, a 3D pyramid, a 2D hexagon and a 2D rectangle. We use a feature number l to characterize the scale of each type of problem, of which the physical meaning is the number of robots on each side of the geometry shape. The relationship between the number of robots n and l is summarized in Table 1. Let $b = 3m$ denote the ground-truth distance between any pair of adjacent robots. The distance measurements are generated according to model (1). The default noise level is $\sigma = 0.10m$. The positions of sensors on each robot are uniformly set as $\bar{v}_i^0 = [0; 0.35m; 0]$ and $\bar{v}_i^1 = [0; -0.35m; 0]$.

One aspect we are concerned about in our setup and optimization model is the sensitivity to initialization. We randomly generate each robot's translation initialization on a ball (for 3D problem) or circle (for 2D problem) with radius r and the robot's translation ground-truth as its center and randomly generate the yaw angle of each robot. A feature value $\rho = \frac{r}{(l-1)b}$ is introduced to indicate the quality of initialization. When ρ is small, we consider it a good initialization, and vice versa a poor initialization. To measure the accuracy of the relative state estimation, we use the average of the root-mean-squared-error (RMSE) for relative translations calculated between each robot and all of its neighbors in the system, which is abbreviated as $RMSE_a$.

We perform all experiments in MATLAB running on a Linux laptop with the Intel i5-11400H. The termination conditions ϵ_F and ϵ in the algorithm are uniformly taken as 5×10^{-3} and 5×10^{-4} respectively in the following experiments. We first empirically determine a reasonable parameter r according to the numerical results in Figure 1. In this experiment, we use poor initializations to trigger failures. We define the failure rate (FR) as the rate at which $RMSE_a$ is greater than 60 cm for 100 experiments. To tradeoff accuracy and efficiency, we believe that it is reasonable to take $d+1$ or $d+3$ for r in 2D problems and d or $d+1$ in 3D problems. In the following experiments, we uniformly take r as $d+1$.

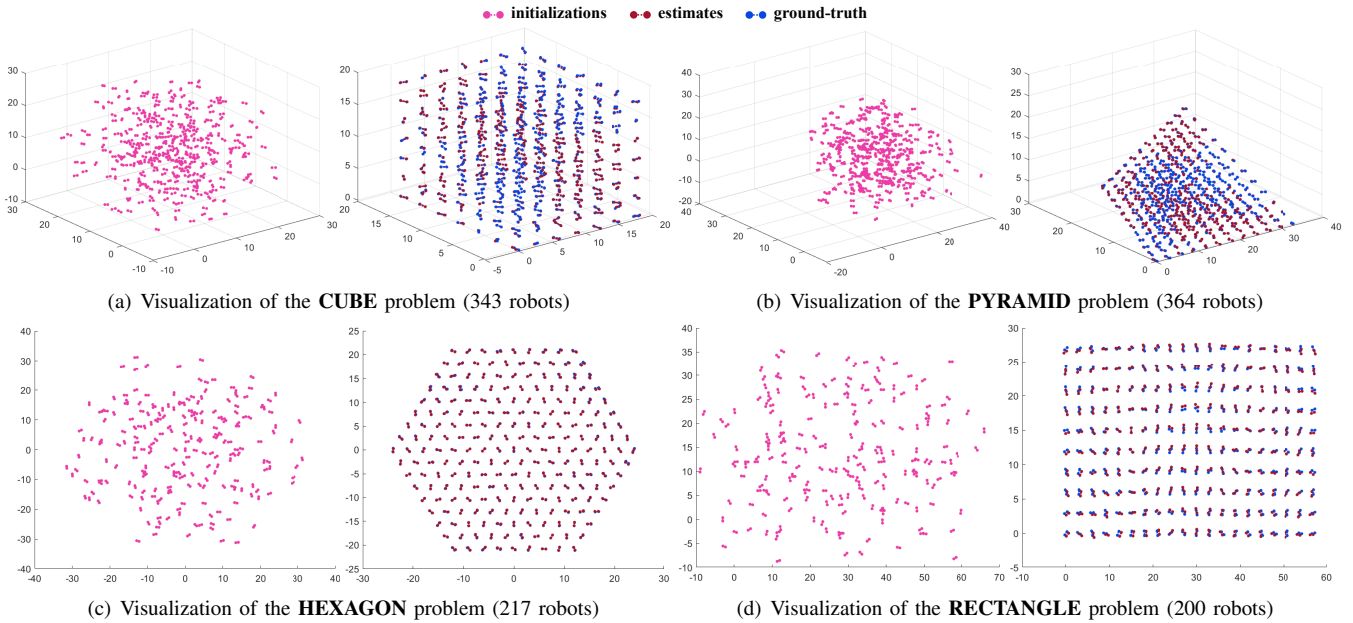


Figure 2. Visualization of the 4 problems with relative poor initializations in Table 2: the two connected balls together with the dotted line connecting them represent a robot, where the balls represent the two sensors on the robot.

A. Results under Varying Noise Levels and Initializations

We comprehensively evaluate the performance of our NLP model with BM-BCD in the four problems at hundreds-scales under different levels of noise contamination and mild versus poor initializations. The results are summarized in Table 2. We use the $(\Delta + 1)$ -coloring algorithm [33] for block division to evaluate the total time (denoted as PT in Table 2) taken to solve the block update subproblem in a parallel and synchronous manner. We also show the total time (denoted as ST in Table 2) to solve each subproblem serially (i.e., in a column-wise block division).

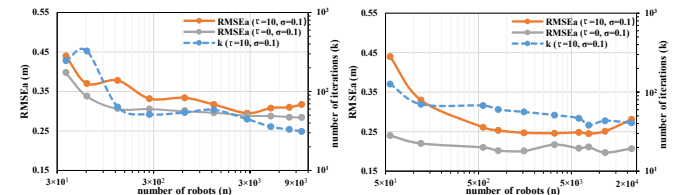
It can be seen from the results that 20-50 cm accuracy is commonly achievable in our setup. The estimates with poor initializations are visualized in Figure 2. The runtime terms in Table 2 show that the algorithm has great potential to achieve real-time performance. The experimental results also showcase the robustness of our proposed model under different initialization conditions, which can be seen from the fact that the results obtained from poor initializations are commonly close to the ones from mild initializations. However, in the **HEXAGON** or **RECTANGLE** problems, poor initialization is more likely to lead to model failure. This may be explained by the low degree of the topology underlying these problems and their realization with *low* rigidity. Low rigidity implies the possibility of ambiguous solutions [3], [15], which is reflected by the more spurious local minima of the NLP model in the presence of noise.

B. Results under Varying System Scales

We evaluate the number of iterations k and the estimation accuracy under initializations with uniform $\tau = 10m$ as the scale increases from dozens to tens of thousands. The results are shown in Figure 3. In this experiment, the estimation accuracy obtained from initializing the model with ground-truth (i.e., $\tau = 0$) is used as a reference, which is approximately considered the accuracy of *global optimal* estimates.

Problem / n	ρ / τ	σ	PT(s) / ST(s) / k / RMSE _a / FR
CUBE / 343	1/4 / 4.5	0.05	0.14 / 1.19 / 40 / 0.13 / 0%
		0.10	0.12 / 1.22 / 45 / 0.25 / 0%
		0.15	0.12 / 1.20 / 42 / 0.37 / 0%
	1/2 / 9	0.05	0.19 / 1.75 / 66 / 0.25 / 2%
		0.10	0.17 / 1.71 / 63 / 0.30 / 2%
		0.15	0.18 / 1.68 / 62 / 0.41 / 3%
PYRAMID / 364	1/6 / 5.5	0.05	0.13 / 1.66 / 43 / 0.15 / 0%
		0.10	0.15 / 1.73 / 47 / 0.25 / 0%
		0.15	0.16 / 1.79 / 49 / 0.37 / 0%
	1/3 / 11	0.05	0.23 / 2.28 / 73 / 0.20 / 0%
		0.10	0.21 / 2.22 / 72 / 0.26 / 0%
		0.15	0.20 / 1.97 / 65 / 0.37 / 1%
HEXAGON / 217	1/4 / 5.25	0.05	0.06 / 0.69 / 70 / 0.15 / 0%
		0.10	0.05 / 0.56 / 58 / 0.28 / 0%
		0.15	0.05 / 0.48 / 51 / 0.45 / 2%
	1/2 / 10.5	0.05	0.08 / 0.84 / 84 / 0.19 / 3%
		0.10	0.09 / 0.78 / 76 / 0.36 / 6%
		0.15	0.06 / 0.68 / 70 / 0.49 / 8%
RECTANGLE / 200	1/4 / 6.75	0.05	0.05 / 0.70 / 75 / 0.22 / 2%
		0.10	0.03 / 0.48 / 62 / 0.37 / 1%
		0.15	0.03 / 0.42 / 56 / 0.55 / 1%
	1/3 / 9	0.05	0.07 / 0.85 / 89 / 0.24 / 4%
		0.10	0.07 / 0.69 / 78 / 0.43 / 7%
		0.15	0.04 / 0.47 / 64 / 0.61 / 8%

Table 2. Numerical results of the proposed model with BM-BCD working on it at varying initializations and noise levels. Statics are computed as the average results under 100 times of data generation for each problem.



(a) RMSE_a and k versus n in **HEXAGON** problems (b) RMSE_a and k versus n in **PYRAMID** problems

Figure 3. Estimation accuracy and number of iterations under varying system scales in 2D and 3D problems.

The experimental results show that in the 2D case, the number of iterations will stabilize (with a slightly decreasing trend) as the system scale increases. When the scale is small, the number of iterations required is significantly higher than that of larger scales. In the 2D case, the estimation accuracy at different scales is close to that of the global optimal estimation in most cases. However, even the global optimal estimation cannot achieve an accuracy of 30 cm at a relatively small scale, reflecting our setup's inherent deficiency. In the 3D cases, the number of iterations with increasing scale shows a similar pattern to the 2D case. Our model always gives estimates with the desired accuracy at a scale of hundreds or thousands in 3D problems. In contrast, the model can not always produce accurate estimates comparable to the global optimal ones at relatively small scales. In the latter cases, even if the estimates seem always to hold a right geometric shape (i.e., the overall shape formed by robots looks like a pyramid), the spatial orientation of the geometry is sometimes wrong.

VI. CONCLUSION AND FUTURE WORKS

This paper proposes an efficient and scalable distributed optimization scheme to handle the distance measurements-based relative state estimation problem. The positive numerical results verify the feasibility of implementing large-scale relative state estimation based on distance measurements. In the future, we plan to find a method for informed initializations to complete our pipeline. Moreover, many (initialization-free) convex relaxation-based schemes have emerged from the study of point realization problems. Combining these techniques to achieve a more robust relative state estimation pipeline would be exciting and promising.

REFERENCES

- [1] S. Bandyopadhyay, S.-J. Chung, and F. Y. Hadaegh, "Probabilistic and distributed control of a large-scale swarm of autonomous agents," *IEEE Transactions on Robotics*, vol. 33, no. 5, pp. 1103–1123, 2017.
- [2] A. Prorok, M. Malencia, L. Carlone, G. S. Sukhatme, B. M. Sadler, and V. Kumar, "Beyond robustness: A taxonomy of approaches towards resilient multi-robot systems," *arXiv preprint arXiv:2109.12343*, 2021.
- [3] M. Shalaby, C. C. Cossette, J. R. Forbes, and J. Le Ny, "Relative position estimation in multi-agent systems using attitude-coupled range measurements," *IEEE Robotics and Automation Letters*, vol. 6, no. 3, pp. 4955–4961, 2021.
- [4] Y. Wang, X. Wen, Y. Cao, C. Xu, and F. Gao, "Bearing-based relative localization for robotic swarm with partially mutual observations," *arXiv preprint arXiv:2210.08265*, 2022.
- [5] C. C. Cossette, M. A. Shalaby, D. Saussié, J. Le Ny, and J. R. Forbes, "Optimal multi-robot formations for relative pose estimation using range measurements," in *2022 IEEE/RSJ International Conference on Intelligent Robots and Systems (IROS)*. IEEE, 2022, pp. 2431–2437.
- [6] B. Jiang, B. D. Anderson, and H. Hmam, "3-d relative localization of mobile systems using distance-only measurements via semidefinite optimization," *IEEE Transactions on Aerospace and Electronic Systems*, vol. 56, no. 3, pp. 1903–1916, 2019.
- [7] T. Ziegler, M. Karrer, P. Schmuck, and M. Chli, "Distributed formation estimation via pairwise distance measurements," *IEEE Robotics and Automation Letters*, vol. 6, no. 2, pp. 3017–3024, 2021.
- [8] T. H. Nguyen and L. Xie, "Relative transformation estimation based on fusion of odometry and ubw ranging data," *arXiv preprint arXiv:2202.00279*, 2022.
- [9] L. Quan, L. Yin, T. Zhang, M. Wang, R. Wang, S. Zhong, Y. Cao, C. Xu, and F. Gao, "Formation flight in dense environments," *arXiv preprint arXiv:2210.04048*, 2022.
- [10] H. Xu, Y. Zhang, B. Zhou, L. Wang, X. Yao, G. Meng, and S. Shen, "Omni-swarm: A decentralized omnidirectional visual-inertial-ubw state estimation system for aerial swarms," *IEEE Transactions on Robotics*, vol. 38, no. 6, pp. 3374–3394, 2022.
- [11] X. Zhou, X. Wen, Z. Wang, Y. Gao, H. Li, Q. Wang, T. Yang, H. Lu, Y. Cao, C. Xu, *et al.*, "Swarm of micro flying robots in the wild," *Science Robotics*, vol. 7, no. 66, p. eabm5954, 2022.
- [12] Z. Han, K. Guo, L. Xie, and Z. Lin, "Integrated relative localization and leader-follower formation control," *IEEE Transactions on Automatic Control*, vol. 64, no. 1, pp. 20–34, 2018.
- [13] A. Fishberg and J. P. How, "Multi-agent relative pose estimation with ubw and constrained communications," in *2022 IEEE/RSJ International Conference on Intelligent Robots and Systems (IROS)*. IEEE, 2022, pp. 778–785.
- [14] Y. Ding, N. Krislock, J. Qian, and H. Wolkowicz, "Sensor network localization, euclidean distance matrix completions, and graph realization," in *Proceedings of the first ACM international workshop on Mobile entity localization and tracking in GPS-less environments*, 2008, pp. 129–134.
- [15] A. M.-C. So and Y. Ye, "Theory of semidefinite programming for sensor network localization," *Mathematical Programming*, vol. 109, no. 2-3, pp. 367–384, 2007.
- [16] P. Biswas, T.-C. Liang, K.-C. Toh, Y. Ye, and T.-C. Wang, "Semidefinite programming approaches for sensor network localization with noisy distance measurements," *IEEE transactions on automation science and engineering*, vol. 3, no. 4, pp. 360–371, 2006.
- [17] Z. Wang, S. Zheng, Y. Ye, and S. Boyd, "Further relaxations of the semidefinite programming approach to sensor network localization," *SIAM Journal on Optimization*, vol. 19, no. 2, pp. 655–673, 2008.
- [18] M. Nishijima and K. Nakata, "A block coordinate descent method for sensor network localization," *Optimization Letters*, vol. 16, no. 3, pp. 1051–1071, 2022.
- [19] G. M. Crippen, T. F. Havel, *et al.*, *Distance geometry and molecular conformation*. Research Studies Press Taunton, 1988, vol. 74.
- [20] P. Biswas, K.-C. Toh, and Y. Ye, "A distributed sdp approach for large-scale noisy anchor-free graph realization with applications to molecular conformation," *SIAM Journal on Scientific Computing*, vol. 30, no. 3, pp. 1251–1277, 2008.
- [21] N.-H. Z. Leung and K.-C. Toh, "An sdp-based divide-and-conquer algorithm for large-scale noisy anchor-free graph realization," *SIAM Journal on Scientific Computing*, vol. 31, no. 6, pp. 4351–4372, 2010.
- [22] D. Bertsekas and J. Tsitsiklis, *Parallel and distributed computation: numerical methods*. Athena Scientific, 2015.
- [23] N. Trawny and S. I. Roumeliotis, "On the global optimum of planar, range-based robot-to-robot relative pose estimation," in *2010 IEEE International Conference on Robotics and Automation*. IEEE, 2010, pp. 3200–3206.
- [24] S. Boyd, L. El Ghaoui, E. Feron, and V. Balakrishnan, *Linear matrix inequalities in system and control theory*. SIAM, 1994.
- [25] S. Mehrotra, "On the implementation of a primal-dual interior point method," *SIAM Journal on optimization*, vol. 2, no. 4, pp. 575–601, 1992.
- [26] S. Burer and R. D. Monteiro, "A nonlinear programming algorithm for solving semidefinite programs via low-rank factorization," *Mathematical Programming*, vol. 95, no. 2, pp. 329–357, 2003.
- [27] Burer, Samuel and Monteiro, Renato DC, "Local minima and convergence in low-rank semidefinite programming," *Mathematical programming*, vol. 103, no. 3, pp. 427–444, 2005.
- [28] B. Jiang and Y.-H. Dai, "A framework of constraint preserving update schemes for optimization on stiefel manifold," *Mathematical Programming*, vol. 153, no. 2, pp. 535–575, 2015.
- [29] J. Nocedal and S. J. Wright, *Numerical optimization*. Springer, 1999.
- [30] Y. Xu and W. Yin, "A block coordinate descent method for regularized multiconvex optimization with applications to nonnegative tensor factorization and completion," *SIAM Journal on imaging sciences*, vol. 6, no. 3, pp. 1758–1789, 2013.
- [31] L. Barenboim and M. Elkin, "Distributed graph coloring: Fundamentals and recent developments," *Synthesis Lectures on Distributed Computing Theory*, vol. 4, no. 1, pp. 1–171, 2013.
- [32] E. T. Hale, W. Yin, and Y. Zhang, "Fixed-point continuation for l_1 -minimization: Methodology and convergence," *SIAM Journal on Optimization*, vol. 19, no. 3, pp. 1107–1130, 2008.
- [33] L. Barenboim, M. Elkin, and F. Kuhn, "Distributed $(\delta+1)$ -coloring in linear (in δ) time," *SIAM Journal on Computing*, vol. 43, no. 1, pp. 72–95, 2014.